Joint Placement and Resource Allocation for UAV-Assisted Mobile Edge Computing Networks with URLLC

ZHANG Pengyu[1], XIE Lifeng[1], XU Jie[2]

(1. School of Information Engineering, Guangdong University of Technology, Guangzhou, Guangdong 510006, China；
2. Future Network of Intelligence Institute and School of Science and Engineering, The Chinese University of Hong Kong, Shenzhen，Guangdong 518172, China)

Abstract: This paper investigates an unmanned aerial vehicle (UAV) assisted mobile edge computing (MEC) network with ultra-reliable and low-latency communications (URLLC), in which a UAV acts as an aerial edge server to collect information from a set of sensors and send the processed data (e.g., command signals) to the corresponding actuators. In particular, we focus on the round-trip URLLC from the sensors to the UAV and to the actuators in the network. By considering the finite block-length codes, our objective is to minimize the maximum end-to-end packet error rate (PER) of these sensor-actuator pairs, by jointly optimizing the UAV's placement location and transmitting power allocation, as well as the users' block-length allocation, subject to the UAV's sum transmitting power constraint and the total block-length constraint. Although the maximum-PER minimization problem is non-convex and difficult to be optimally solved, we obtain a high-quality solution to this problem by using the technique of alternating optimization. Numerical results show that our proposed design achieves significant performance gains over other benchmark schemes without the joint optimization.

Keywords: UAV; MEC; URLLC; placement optimization; resource allocation

Citation (IEEE Format): P. Y. Zhang, L. F. Xie, J. Xu, et al., "Joint placement and resource allocation for UAV-assisted mobile edge computing networks with URLLC," *ZTE Communications*, vol. 18, no. 2, pp. 49 – 56, Jun. 2020. doi: 10.12142/ZTECOM.202002007.

1 Introduction

Recent advances in artificial intelligence (AI) and Internet of Things (IoT) are envisioned to enable various new intelligent applications such as augmented reality (AR), virtual reality (VR), and unmanned aerial vehicles (UAVs). Towards this end, billions of IoT devices (e.g., smart sensors and actuators) will be deployed in future wireless networks to collect information from the environments and take physical actions, and machine learning functionalities will be incorporated into wireless networks to analyze and acquire knowledge from these data for making decisions. In this case, how to provide real-time sensing, communication, and control among a large number of sensors and actuators, and how to implement real-time machine learning in the loop are challenging issues in the design of beyond-fifth-generation (B5G) or sixth-generation (6G) cellular networks towards a vision of network intelligence.

Mobile edge computing (MEC)[1 – 7] and learning[8 – 10] have

emerged as important techniques to deal with the above issues, by pushing the cloud-like computation and storage capabilities, and the machine learning functionality at the network edge, e. g., base stations (BSs) and access points (APs). Accordingly, the edge servers at BSs/APs can help end users remotely execute the computation-intensive applications in a swift way, and quickly acquire knowledge from the locally generated data at IoT devices for making quick decisions. However, wireless communications among end devices and BSs/APs are becoming the performance bottleneck for such systems, as the wireless channels connecting them may fluctuate over time and be unstable. Prior works have investigated the joint communication and computation design for mobile edge computing[1 – 4] and for training in mobile edge learning[8 – 10], respectively. Besides the joint design of communication and computation, the ultra-reliable and low-latency round-trip communications from sensors to edge servers and to actuators are another crucial issue for successfully implementing the machine edge learning with critical latency requirements. For instance, consider the inference phase in mobile edge learning, where trained machine learning models are deployed at the edge server. In this case, IoT devices[11] (e.g., sensors) first send the sensed information to the edge server; after receiving such information, the edge server implements the inference process and sends the inference results (e. g., such as command signals) back to the same or other IoT devices (e.g., actuators) for taking actions. In this scenario, the round-trip ultra-reliable and low-latency communications (URLLC) for the "sensors-edge-server-actuators" flow is important and thus is the main focus of this paper.

Furthermore, UAV-assisted wireless platforms[12 – 14] are promising techniques towards B5G. UAV-assisted wireless platforms can provide flexible wireless services to on-ground devices by deploying wireless transceivers (such as BSs and APs) at UAVs that can fly freely over the three-dimensional (3D) space. Compared with conventional terrestrial wireless infrastructures, UAV-enabled BSs/APs are advantageous due to their deployment flexibility, strong line of sight (LoS) channels with on-ground users, and highly controllable mobility[15 – 18]. By exploiting the controllable mobility, the UAVs can fly closer to intended on-ground devices and fly farther away from unintended ones to help enhance the communication performance. By integrating UAVs with MEC, UAV-enabled MEC has attracted a lot of recent research interests, in which the UAV is deployed as dedicated aerial MEC server to support the communication and computation of end users on the ground. Prior works have investigated the computation offloading design in the UAV-assisted MEC, in which wireless devices (such as smartphones) offload their own computation tasks to the UAV for enhancing the performance of task execution[13], [19 – 24]. For instance, Refs. [22] and [23] aim to minimize the energy consumption of the UAV while ensuring the quality of service (QoS) requirements at users, by jointly optimizing

the UAV's flight and wireless resource allocation. Refs. [19] and [24] optimize the flight trajectory and communication wireless resource allocation at the UAV, so as to maximize the UAV's endurance time or communication rate.

Different from prior works, this paper focuses on the round-trip URLLC in mobile edge networks, in which the UAV-enabled edge server is employed to improve the round-trip communication performance from on-ground sensors to the UAV and to the actuators. This may practically correspond to a delay-sensitive inference scenario in mobile edge learning, where the machine learning models are deployed at the UAV for remote control. To our best knowledge, the problem of round-trip URLLC under this scenario has not been addressed yet. This problem, however, is challenging to be dealt with. First, for achieving URLLC, the delivered packets (e. g., the sensed information by the sensors and the command signals sent from the MEC server to the actuators) are generally with small block lengths, and as a result, the conventional Shannon capacity under the assumptions of infinite block length and zero decoding error is not applicable. Therefore, we must take into account the effect of finite block-length codes, under which new performance metrics characterizing the relations among the communication rate, packer error rate (PER), and block-length should be considered[25 – 26]. Next, there generally exist a large number of sensors and actuators over IoT networks. It is thus very important to efficiently design wireless resource allocation among these sensor-actuator pairs. This, however, is technically very difficult due to the new performance metrics considered. Last but not least, the UAVs' mobility can be exploited via trajectory control[24] or deployment optimization[27] for optimizing the MEC performance. How to jointly design the UAVs' deployment optimization or trajectory control together with the wireless resource allocation is also a new problem to be tackled for URLLC.

Notice that Ref. [27] studies the UAV-enabled relaying system with URLLC, in which the UAV's deployment location and the block-length allocation are jointly optimized, for the purpose of minimizing the end-to-end PER from the ground source node to the ground destination node. In contrast to Ref. [27] that focused on the relaying scenario with only one single source-destination pair, this paper studies a different UAV-enabled MEC scenario with multiple sensor-actuator pairs, for which both the transmitting power allocation at the UAV and the block-length allocation are considered, together with the UAV's deployment optimization.

This paper investigates a UAV-assisted MEC network with URLLC as shown in **Fig. 1**, in which a single UAV acts as an aerial edge server to collect information sent from multiple sensors, analyze such information (via, e.g., machine learning), and then send the processed data (e.g., command signals) to their respective actuators. We focus our study on the round-trip URLLC by assuming the time and resource consumption for information processing at the UAV which is given and thus ig-
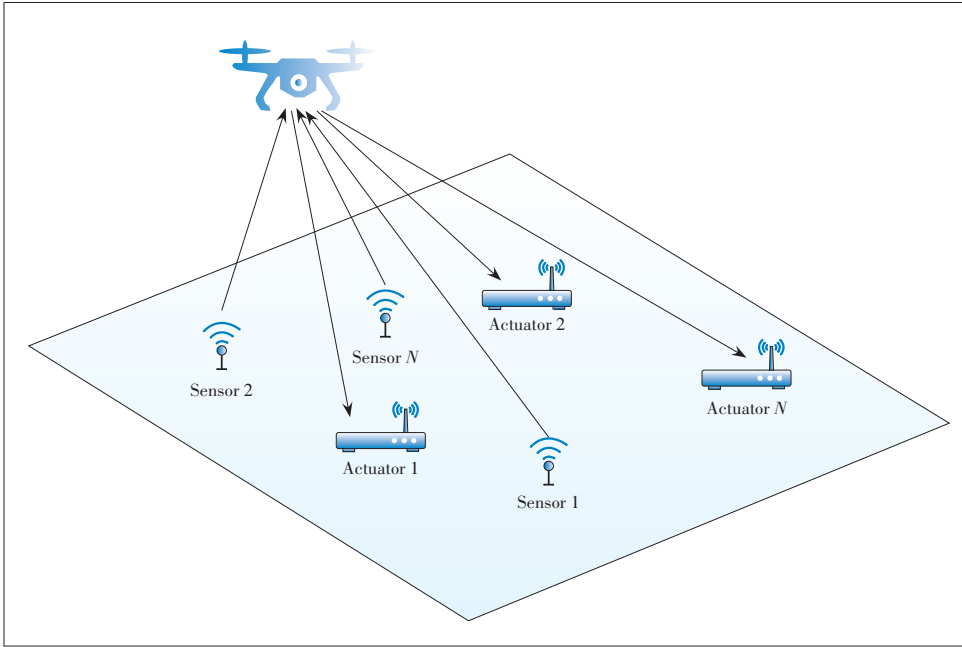
▲ Figure 1. Unmanned aerial vehicle (UAV) assisted mobile edge computing (MEC) network with one UAV acting as an MEC server to serve multiple sensors and actuators on the ground.

nored. Furthermore, we consider the quasi-stationary UAV scenario[1], in which the UAV hovers at an optimized location during the whole communication period of our interest. The main results of this paper are summarized as follows.

• Under the above setup, we aim to minimize the maximum end-to-end PER of these sensor-actuator pairs, by jointly optimizing the UAV's placement location and wireless resource allocation, subject to the UAV's sum transmitting power constraint and the total block-length constraint.

• The formulated problem is non-convex and thus is difficult to be solved optimally. To tackle this difficulty, we propose an alternating-optimization-based algorithm to obtain a high-quality solution, in which the UAV's placement location and transmitting power allocation and the users' block-length allocation are optimized in an alternating manner.

• Numerical results are provided to validate the performance of our proposed UAV-enabled round-trip URLLC among multiple sensor-actuator pairs. It is shown that our proposed design achieves much lower PER than other benchmark schemes without such joint optimization. It is also shown that when the transmitting power at the UAV becomes large, proper wireless resource allocation among different sensor-actuator pairs is crucial to enhance the maximum PER performance.

The remainder of this paper is organized as follows. Section 2 introduces the system model of the UAV-assisted MEC network with URLLC, and formulates the maximum-PER minimization problem of our interest. Section 3 proposes an efficient algorithm to obtain a high-quality solution to the formulated problem by using the alternating optimization and the Lagrange duality method. Section 4 presents numerical results to validate

the performance of our proposed approaches. Finally, Section 5 concludes this paper.

2 System Model

As shown in Fig. 1, a UAV-assisted MEC network, in which a UAV is dispatched as an aerial MEC server to serve N pairs of sensors and actuators, is considered. We use $\mathcal{N} = \{1,...,N\}$ to denote the set of sensors or actuators. In particular, the UAV collects information sent from the N sensors in the uplink and then transmits the processed data (or command signals) to the respective actuators in the downlink. Suppose that the sensor $i \in \mathcal{N}$ and actuator $i \in \mathcal{N}$ on the ground have fixed locations $(\hat{x}_i, \hat{y}_i, 0)$ and $(\tilde{x}_i, \tilde{y}_i, 0)$ in a 3D Cartesian coordinate system, where $\hat{\mathbf{w}}_i = (\hat{x}_i, \hat{y}_i)$ and $\tilde{\mathbf{w}}_i = (\tilde{x}_i, \tilde{y}_i)$ are defined as their horizontal coordinates, respectively. The locations of sensors and actuators are assumed to be a-priori known by the UAV to facilitate the placement location optimization and wireless resource allocations.

The UAV is assumed to stay at a fixed altitude H above the ground, and the horizontal coordinate of the UAV is denoted by $\mathbf{q} = (x, y)^2$. Therefore, the distance from the UAV to sensor i and actuator i are respectively given as:

$$\hat{d}_i = \sqrt{H^2 + \|\mathbf{q} - \hat{\mathbf{w}}_i\|^2}, \forall i \in \mathcal{N}, \tag{1}$$

$$\tilde{d}_i = \sqrt{H^2 + \|\mathbf{q} - \tilde{\mathbf{w}}_i\|^2}, \forall i \in \mathcal{N}, \tag{2}$$

where $\|\cdot\|$ denotes the Euclidean norm of a vector.

It is assumed that the wireless channels from the UAV to ground sensors or actuators are dominated by LoS links. Thus, the channel power gained from the UAV to sensor i and actuator i follows the free-space path loss model, which is expressed as:

$$\hat{h}_i(\mathbf{q}) = \rho_0 \hat{d}_i^{-2} = \frac{\rho_0}{H^2 + \|\mathbf{q} - \hat{\mathbf{w}}_i\|^2}, \forall i \in \mathcal{N}, \tag{3}$$

---

1 There is another scenario, namely the fully-mobile UAV scenario, in which the UAV can fly around over the communication period and thus the trajectory control becomes crucial. Note that in our considered setup, the on-ground sensors and actuators are at fixed locations. Therefore, we only consider the quasi-stationary UAV scenario by optimizing the deployment location only.

2 In this paper, we assume that the UAV hovers at an unchanged location during the whole flight period.

$$\tilde{h}_i(\boldsymbol{q}) = \rho_0 \tilde{d}_i^{-2} = \frac{\rho_0}{H^2 + \|\boldsymbol{q} - \tilde{\boldsymbol{w}}_i\|^2}, \forall i \in \mathcal{N}, \tag{4}$$

where ρ_0 denotes the channel power gained at the reference distance of $d_0 = 1$ m.

In the uplink, each sensor adopts constant power Q to send messages to the UAV. In this case, the correspondingly received signal-to-noise-ratio (SNR) at the UAV can be expressed as:

$$\hat{\gamma}_i(\boldsymbol{q}) = \frac{Q\hat{h}_i(\boldsymbol{q})}{\sigma^2}, \forall i \in \mathcal{N}. \tag{5}$$

In the downlink, the UAV adopts transmitting power $p_i, i \in \mathcal{N}$ to send the processed data to actuator i. Thus, the correspondingly received SNR at actuator i can be expressed as:

$$\tilde{\gamma}_i(\boldsymbol{q}, p_i) = \frac{p_i \tilde{h}_i(\boldsymbol{q})}{\sigma^2}, \forall i \in \mathcal{N}, \tag{6}$$

where σ^2 denotes the power of the additive white Gaussian noise (AWGN) at the receiver. Suppose that the UAV's downlink transmission power is P_{sum}. Then we have $\sum_{i \in N} p_i \leqslant P_{\text{sum}}$.

We consider the time-division multiple access (TDMA) transmission protocol, in which the uplink transmission from each sensor to the UAV and the downlink transmission from the UAV to each actuator are implemented over the same frequency band and orthogonal time instants. Suppose that the size of the packet generated by sensor i is denoted as $\hat{k}_i$ and that desired by actuator i is denoted as $\tilde{k}_i$, which are generally different. Accordingly, let $\tilde{m}_i$ and $\hat{m}_i$ denote the allocated block-length during the uplink and downlink transmission for the i-th sensor-actuator pair, $i \in \mathcal{N}$, respectively. Thus, we have $\sum_{i=1}^{N} (\hat{m}_i + \tilde{m}_i) \leqslant M$, where M denotes the total block-length.

In order to process the uploaded data from sensors, the UAV needs to consume certain time and energy for implementing the inference task. Let f and κ denote the CPU frequency and the effective capacitance for computing at the UAV, C denote the total CPU cycles required for accomplishing the task. Then the energy required for executing the inference task is approximated $P_{\text{comp}} = \kappa C f^2$ and the time duration for computation is given as T_{comp}[13]. Suppose that δ is the symbol length for wireless communication and T_{total} denotes the total end-to-end delay for the inference task. Then we have $\delta M = T_{\text{total}} - T_{\text{comp}}$. In this paper, we assume that the computation delay T_{comp} and energy consumption P_{comp} are given and thus are not considered in the optimization of our interest.

Based on the achievable rate formula of finite block-length codes[25], it follows that to transmit a short packet within finite symbols, the PERs (within (0, 0.5)) of the uplink and downlink transmission for the i-th sensor-actuator pairs are approximat-

ed as the following two formulas, respectively[25].

$$\hat{\varepsilon}_i(\hat{k}_i, \boldsymbol{q}, \hat{m}_i) = Q\left(\frac{\hat{m}_i \ln(1 + \hat{\gamma}(\boldsymbol{q})) - \hat{k}_i \ln 2}{\sqrt{\hat{m}_i} \sqrt{1 - (1 + \hat{\gamma}(\boldsymbol{q}))^{-2}}}\right), \tag{7}$$

$$\tilde{\varepsilon}_i(\tilde{k}_i, \boldsymbol{q}, \tilde{m}_i) = Q\left(\frac{\tilde{m}_i \ln(1 + \tilde{\gamma}(\boldsymbol{q})) - \tilde{k}_i \ln 2}{\sqrt{\tilde{m}_i} \sqrt{1 - (1 + \tilde{\gamma}(\boldsymbol{q}))^{-2}}}\right), \tag{8}$$

where $Q(x) = \frac{1}{\sqrt{2\pi}} \int_x^{\infty} e^{-\frac{t^2}{2}} dt$.

As a result, we define the end-to-end PER of the i-th sensor-actuator pair as the rate when the packet error occurs at either the uplink or downlink transmission, which is denoted as ε_i and given by

$$\varepsilon_i = 1 - (1 - \hat{\varepsilon}_i(\hat{k}_i, \boldsymbol{q}, \hat{m}_i))(1 - \tilde{\varepsilon}_i(\tilde{k}_i, \boldsymbol{q}, \tilde{m}_i)) = \\ \hat{\varepsilon}_i(\hat{k}_i, \boldsymbol{q}, \hat{m}_i) + \tilde{\varepsilon}_i(\tilde{k}_i, \boldsymbol{q}, \tilde{m}_i) - \hat{\varepsilon}_i(\hat{k}_i, \boldsymbol{q}, \hat{m}_i) \times \tilde{\varepsilon}_i(\tilde{k}_i, \boldsymbol{q}, \tilde{m}_i). \tag{9}$$

In general, under our URLLC consideration, the sensor-actuator pairs should work at the regime when the PERs are generally very small, i.e., it should hold that $\hat{\varepsilon}_i(\hat{k}_i, \boldsymbol{q}, \hat{m}_i) \leqslant 10^{-1}$, $\tilde{\varepsilon}_i(\tilde{k}_i, \boldsymbol{q}, \tilde{m}_i) \leqslant 10^{-1}, i \in \mathcal{N}$. In this case, we have $\hat{\varepsilon}_i(\hat{k}_i, \boldsymbol{q}, \hat{m}_i) + \tilde{\varepsilon}_i(\tilde{k}_i, \boldsymbol{q}, \tilde{m}_i) \gg \hat{\varepsilon}_i(\hat{k}_i, \boldsymbol{q}, \hat{m}_i) \times \tilde{\varepsilon}_i(\tilde{k}_i, \boldsymbol{q}, \tilde{m}_i)$, and accordingly, it follows that $\varepsilon_i \approx \hat{\varepsilon}_i(\hat{k}_i, \boldsymbol{q}, \hat{m}_i) + \tilde{\varepsilon}_i(\tilde{k}_i, \boldsymbol{q}, \tilde{m}_i), \forall i \in \mathcal{N}$[27].

Our objective is to minimize the maximum PER of the N pairs, by jointly optimizing the UAV's placement location and transmitting power allocation, and the users' block-length, subject to the total block-length constraint and the sum transmitting power constraint at the UAV. For notational convenience, we denote that $\boldsymbol{m} \triangleq \{\hat{m}_i, \tilde{m}_i\}$, $\boldsymbol{p} \triangleq \{p_i\}$. Therefore, the maximum end-to-end PER minimization problem of our interest can be formulated as

$$(\text{P1}): \min_{\boldsymbol{q}, \boldsymbol{m}, \boldsymbol{p}} \quad \max_{i \in N} \hat{\varepsilon}_i(\hat{k}_i, \boldsymbol{q}, \hat{m}_i) + \tilde{\varepsilon}_i(\tilde{k}_i, \boldsymbol{q}, \tilde{m}_i)$$

$$\text{s.t.} \; \hat{\varepsilon}_i(\hat{k}_i, \boldsymbol{q}, \hat{m}_i) < 10^{-1}, \tilde{\varepsilon}_i(\tilde{k}_i, \boldsymbol{q}, \tilde{m}_i) < 10^{-1}, \forall i \in \mathcal{N} \tag{10a}$$

$$\sum_{i \in N} (\hat{m}_i + \tilde{m}_i) \leqslant M \tag{10b}$$

$$\sum_{i \in N} p_i \leqslant P_{\text{sum}} \tag{10c}$$

$$p_i \geqslant 0, \forall i \in \mathcal{N}, \tag{10d}$$

where Eq. (10a) corresponds to the constraints for the approximation of objective function to be accurate, Eq. (10b) denotes the total block-length constraint and Eq. (10c) denotes the sum transmitting power constraint at the UAV. As the objective function in (P1) is a non-convex function in general, the problem (P1) is a non-convex problem that is generally difficult to be optimally solved.

3 Proposed Solution to Problem (P1)

In this section, we propose an efficient algorithm to obtain a high-quality solution to the problem (P1). Towards this end, we first introduce an auxiliary variable ε, and equivalently reformulate the problem (P1) as

(P2): $\min\limits_{q,m,p,\varepsilon}$ ε

s.t. $\hat{\varepsilon}_i(\hat{k}_i, q, \hat{m}_i) + \tilde{\varepsilon}_i(\tilde{k}_i, q, \tilde{m}_i) \leq \varepsilon, \forall i \in \mathcal{N}$ (11)

(10a), (10b) and (10c).

However, the problem (P2) is still non-convex. To tackle this challenge, we propose an algorithm to solve the problem (P2) or (P1) by using the alternating optimization technique, in which the block-length allocation, the transmitting power allocation, and the deployment location are optimized in an alternating manner, by considering the others to be given, towards a converged solution.

3.1 Block-Length Allocation

Under any given UAV's location q and power allocation p, the block-length allocation problem is formulated as

(P2.1): $\min\limits_{m,\varepsilon}$ ε

s.t. $\hat{\varepsilon}_i(\hat{k}_i, q, \hat{m}_i) + \tilde{\varepsilon}_i(\tilde{k}_i, q, \tilde{m}_i) \leq \varepsilon, \forall i \in \mathcal{N}$,   (12a)

$\sum\limits_{i \in \mathcal{N}} (\hat{m}_i + \tilde{m}_i) \leq M$.   (12b)

Since the error rate functions $\varepsilon(k, q, m)$ in the constraint (12a) are convex with respect to m[26], the problem (P2.1) is a convex optimization problem. Therefore, the strong duality holds between (P2.1) and its Lagrange dual problem. As a result, we can optimally solve (P2.1) by using the Lagrange duality method[28].

Let $\lambda_i \geq 0, \forall i \in \mathcal{N}$ and $\mu \geq 0$ denote the dual variables associated with the i-th constraint in Eqs. (12a) and (12b), respectively. Then we define $\boldsymbol{\lambda} \triangleq [\lambda_1,...,\lambda_N]$. Let $\mathcal{X}$ denote the set $\boldsymbol{\lambda}$ and μ specified by the constraints in the dual problem of (P2.1). The Lagrangian of problem (P2.1) is given by

$\mathcal{L}_1(\varepsilon, \boldsymbol{m}, \boldsymbol{\lambda}, \mu) = (1 - \sum\limits_{i \in N} \lambda_i)\varepsilon + \sum\limits_{i \in N} \lambda_i (\hat{\varepsilon}_i(\hat{k}_i, q, \hat{m}_i) +$
$\tilde{\varepsilon}_i(\tilde{k}_i, q, \tilde{m}_i)) + \mu \sum\limits_{i \in N} (\hat{m}_i + \tilde{m}_i) - \mu M.$ (13)

Accordingly, the dual function of (P2.1) is

$g(\boldsymbol{\lambda}, \mu) = \min\limits_{m,\varepsilon} L(\boldsymbol{m}, \varepsilon, \boldsymbol{\lambda}, \mu)$
s.t. (12a) and (12b).   (14)

As a result, the dual problem is given by

(D2.1): $\max\limits_{\lambda,\mu}$ $g(\boldsymbol{\lambda}, \mu)$

s.t. $\sum\limits_{i=1}^{N} \lambda_i = 1$ (15)

$\mu \geq 0, \lambda_i \geq 0, \forall i \in \mathcal{N}.$

First, we obtain the dual function under any given $\boldsymbol{\lambda}$ and μ by solving Eq. (14). Towards this end, we obtain the optimal solution $\{\tilde{m}_i^*\}$ and $\{\hat{m}_i^*\}$ via solving Eqs. (16) and (17) by using a bisection search.

$\frac{\partial \mathcal{L}_1}{\partial \tilde{m}_i} = \lambda_i \frac{-(\tilde{a}\tilde{m}_i + \tilde{b})}{2\sqrt{2\pi} \tilde{m}_i^{3/2}} e^{-(\tilde{a}\sqrt{\tilde{m}_i} - \tilde{b}/\sqrt{\tilde{m}_i})^2/2} + \mu = 0,$ (16)

$\frac{\partial \mathcal{L}_1}{\partial \hat{m}_i} = \lambda_i \frac{-(\hat{a}\hat{m}_i + \hat{b})}{2\sqrt{2\pi} \hat{m}_i^{3/2}} e^{-(\hat{a}\sqrt{\tilde{m}_i} - \hat{b}/\sqrt{\tilde{m}_i})^2/2} + \mu = 0,$ (17)

where $\tilde{a} = \dfrac{\ln(1 + \tilde{\gamma}_i)}{\sqrt{1 - (1 + \tilde{\gamma}_i)^{-2}}} > 0$ and $\tilde{b} = \dfrac{k\ln 2}{\sqrt{1 - (1 + \tilde{\gamma}_i)^{-2}}} > 0$.

Then, we obtain the optimal $\boldsymbol{\lambda}^{\text{opt}}$ and μ^{opt} via solving the dual problem (D2.1) by using sub-gradient based method[29], such as the ellipsoid method. With $\boldsymbol{\lambda}^{\text{opt}}$ and μ^{opt} at hand, we can obtain the optimal solution $\{\tilde{m}_i^{\text{opt}}\}$ and $\{\hat{m}_i^{\text{opt}}\}$ by replacing $\boldsymbol{\lambda}$ and μ in Eqs. (16) and (17) as $\boldsymbol{\lambda}^{\text{opt}}$ and μ^{opt}. Therefore, problem (P2.1) is solved.

3.2 Power Allocation

For any given UAV's location q and block-length allocation m, the power allocation problem is formulated as:

(P 2.2): $\min\limits_{p,\varepsilon}$ ε

s.t. $\hat{\varepsilon}_i(\hat{k}_i, q, \hat{m}_i) + \tilde{\varepsilon}_i(\tilde{k}_i, q, \tilde{m}_i) \leq \varepsilon, \forall i \in \mathcal{N}$ (18a)

$\sum\limits_{i \in N} p_i \leq P_{\text{sum}}$ (18b)

$p_i \geq 0, \forall i \in \mathcal{N}.$ (18c)

We have the following lemma for solving the problem.

Lemma: For any given UAV's location q and latency allocation m, the error rate ε is convex in p under the mild condition $\varepsilon(\gamma, m) < 0.5$.

Proof: See Appendix.

Since the error rate functions $\varepsilon(k, q, m)$ in the constraint (18a) are convex with respect to p, the problem (P2.2) is a convex optimization problem. Therefore, the strong duality also holds between (P2.2) and its Lagrange dual problem. As a result, we can optimally solve (P2.2) by using Lagrange duality method.

Let $\zeta_i \geq 0, \nu_i \geq 0, \forall i \in \mathcal{N}$, and $\eta \geq 0$ denote the dual variables associated with the constraints (18a), (18c) and (18b), re-

spectively. Then we define $\boldsymbol{\zeta} \triangleq [\zeta_1,...,\zeta_N]$ and $\boldsymbol{\nu} \triangleq [\nu_1,...,\nu_N]$. Let $\boldsymbol{\gamma}$ denote the set of $\boldsymbol{\zeta}$, $\boldsymbol{\eta}$ and $\boldsymbol{\nu}$ specified by the constraints in the dual problem of (P2.2). The Lagrangian of the problem (P2.2) is given by

$$\mathcal{L}_2(\boldsymbol{p},\varepsilon,\boldsymbol{\zeta},\boldsymbol{\nu},\boldsymbol{\eta}) = (1 - \sum_{i \in N}\zeta_i)\varepsilon + \sum_{i \in N}\zeta_i\ (\hat{\varepsilon}_i(\hat{k}_i,\boldsymbol{q},\hat{m}_i) + \tilde{\varepsilon}_i(\tilde{k}_i,\boldsymbol{q},\tilde{m}_i)) + \eta\sum_{i \in N}p_i - \sum_{i \in N}\nu_i\,p_i - \eta P_{\text{sum}}. \quad (19)$$

Accordingly, the dual function is given as:

$$g(\boldsymbol{\zeta},\boldsymbol{\nu},\boldsymbol{\eta}) = \min_{\boldsymbol{p},\varepsilon}\ \ L(\boldsymbol{p},\varepsilon,\boldsymbol{\zeta},\boldsymbol{\nu},\boldsymbol{\eta}) \\ \text{s.t.}\ \ (18a),(18b)\ \text{and}\ (18c). \quad (20)$$

As a result, the dual problem of (P2.2) is expressed as

$$(\text{D2.2}): \max_{\varsigma,\mu,\varphi}\ \ g(\boldsymbol{\zeta},\boldsymbol{\nu},\boldsymbol{\eta})$$

$$\text{s.t.}\ \ \sum_{i=1}^N\zeta_i = 1 \quad (21)$$

$$\eta \geqslant 0, \zeta_i \geqslant 0, \nu_i \geqslant 0, \forall i \in \mathcal{N}.$$

First, we obtain the dual function of Eq. (20) under any given $\boldsymbol{\zeta}$, $\boldsymbol{\eta}$ and $\boldsymbol{\nu}$ by solving the problem of Eq. (22). In particular, we can obtain the optimal solution $\{p_i^*\}$ via solving Eq. (22) by the bisection search.

$$\frac{\partial\mathcal{L}_2}{\partial p_i} = \frac{\zeta_i}{\sqrt{2\pi}}A_d e^{(-A^2)/2} + \eta - \nu_i = 0, \quad (22)$$

where

$$A_d \triangleq \frac{-(\dfrac{\dfrac{h}{\sigma^2}m^{3/2}\sqrt{1-(1+\gamma_i)^{-2}}}{1+\gamma_i} - \dfrac{\sqrt{m}\dfrac{h}{\sigma^2}(m\ln(1+\gamma_i)-k\ln2)}{(1+\gamma_i)^3\sqrt{1-(1+\gamma_i)^{-2}}})}{m(1-(1+\gamma_i)^{-2})}, \quad (23)$$

$$A \triangleq \frac{m\ln(1+\gamma_i)-k\ln2}{\sqrt{m}\sqrt{1-(1+\gamma_i)^{-2}}}. \quad (24)$$

Then we obtain the optimal $\boldsymbol{\zeta}^{\text{opt}}$, $\boldsymbol{\eta}^{\text{opt}}$ and $\boldsymbol{\nu}^{\text{opt}}$ via solving the dual problem (D2.2) by using the ellipsoid method[28]. With $\boldsymbol{\zeta}^{\text{opt}}$, $\boldsymbol{\eta}^{\text{opt}}$ and $\boldsymbol{\nu}^{\text{opt}}$ obtained, we can determine the optimal solution $\{p_i^{\text{opt}}\}$ by replacing $\boldsymbol{\zeta}, \boldsymbol{\eta}$ and $\boldsymbol{\nu}$ in Eq. (22) as $\boldsymbol{\zeta}^{\text{opt}}$, $\boldsymbol{\eta}^{\text{opt}}$ and $\boldsymbol{\nu}^{\text{opt}}$. Therefore, problem (P2.2) is finally solved.

3.3 UAV Placement Optimization

Finally, under any given UAV's transmitting power allocation $\boldsymbol{p}$ and users' block-length allocation $\boldsymbol{m}$, we optimize the UAV placement location, for which the optimization problem is formulated as

$$(\text{P2.3}): \min_{x,y,\varepsilon}\ \ \varepsilon$$

$$\text{s.t.}\ \ \hat{\varepsilon}_i(\hat{k}_i,\boldsymbol{q},\hat{m}_i) + \tilde{\varepsilon}_i(\tilde{k}_i,\boldsymbol{q},\tilde{m}_i) \leqslant \varepsilon, \forall i \in \mathcal{N}. \quad (25)$$

We solve the problem (P2.3) by adopting a two-dimensional (2D) exhaustive search over the region $[\underline{x},\overline{x}] \times [\underline{y},\overline{y}]$, where $\underline{x} = \min_{i \in \mathcal{N}}(\hat{x}_i,\tilde{x}_i)$, $\overline{x} = \max_{i \in \mathcal{N}}(\hat{x}_i,\tilde{x}_i)$, $\underline{y} = \min_{i \in \mathcal{N}}(\hat{y}_i,\tilde{y}_i)$, $\overline{y} = \max_{i \in \mathcal{N}}(\hat{y}_i,\tilde{y}_i)$.

In summary, we optimize the UAV's placement location $\boldsymbol{q}$ and the wireless resource allocation $\boldsymbol{m}$ and $\boldsymbol{p}$ in an alternating manner. It is worth noting that the objective value (i. e., the achieved maximum end-to-end PER value) is monotonically non-increasing after each update. As a result, the alternating-optimization-based approach eventually converges to a converged solution to (P2) or (P1), as the maximum PER value is lower bounded by zero. It is also worth noting that the proposed algorithm can be employed offline before the UAV is launched for helping perform the inference task, which can thus be implemented efficiently in practice and will not affect the low latency requirement of the online computation task.

4 Numerical Results

In this section, we present numerical results to evaluate the performance of the proposed design. In the simulation, we randomly generate sensors and actuators' positions in a 2D area within $100 \times 100\ \text{m}^2$. We set $\hat{k}_i =100$ bit and $\tilde{k}_i =80$ bit, and $\forall i \in \mathcal{N}$ for uplink and downlink communications. The reference channel power gain is set as $\rho_0 = -40$ dB and the receiver noise power is $\sigma^2 = -90$ dBm. The transmitting power of all sensors is Q = 1 W. The UAV flies at a fixed altitude of H = 120 m. We consider the following reference schemes for performance comparison.

• **Benchmark scheme**: In this scheme, the UAV hovers above a fixed location (i. e., the middle point of the area) and wireless resources are allocated equally among all sensor-actuator pairs (i. e., $\dfrac{M}{2N}$ for all the sensor-actuator pairs' block-length and $\dfrac{P_{\text{sum}}}{N}$ for the UAV's transmitting power to actuators).

•**Placement optimization only**: In this scheme, we consider equal block-length and power allocations (i. e., wireless resources are allocated to all the sensor-actuator pairs evenly). Under this design, the UAV hovers at an optimized location, which can be obtained by solving the problem (P2.3) under given UAV's transmitting power allocation $\boldsymbol{p}$ and users' block-length allocation $\boldsymbol{m}$.

• **Resource allocation only**: The UAV hovers above the middle point of the area with optimal wireless resource allocations, which can be obtained via solving the problems (P2.1) and (P2.2).

Fig. 2 shows the maximum end-to-end PER versus the total block-length M, where we set $P_{\text{sum}} = 36$ dBm. It is observed

that our proposed design outperforms other reference schemes and the performance gain becomes more significant when the total block-length becomes larger. It is also observed that the resource allocation only scheme significantly outperforms the placement optimization only scheme. This shows the importance of the joint uplink and downlink resource allocation.
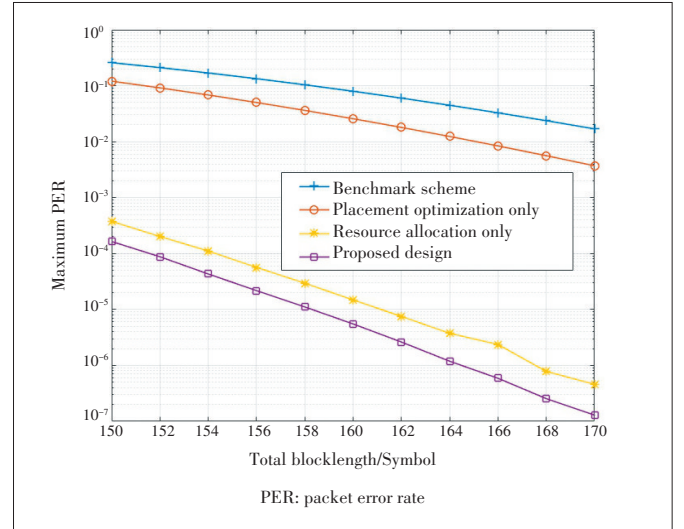
Fig. 3 shows the maximum end-to-end PER versus the total transmitting power P_{sum}, where we set $M = 150$. It is observed that the scheme with placement optimization only and the benchmark scheme both lead to a PER error floor when $P_{sum} >$ 33 dBm. It is also observed that in the low transmitting power regime, the placement only scheme slightly outperforms the resource allocation only scheme. By contrast, when the transmitting power becomes high, the placement only scheme and the benchmark scheme result in unchanged maximum PER values, which is due to the fact that the PER performance is fundamentally limited by the uplink because of the lacking of resource allocations. In this case, the resource allocation only scheme and the proposed design lead to monotonically decreasing maximum PER values as transmitting power increases. Over all transmitting power regimes, the proposed design with both resource allocation and UAV placement optimization is observed to always achieve the best performance, and the performance gain becomes more evident when the transmitting power becomes larger.

5 Conclusions

In this paper, we study a new UAV-assisted MEC network with URLLC, in which a UAV is deployed at an optimizable location for serving multiple pairs of sensors and actuators. We minimize the maximum end-to-end PER of these sensor-actuator pairs by jointly optimizing the UAV's placement location and transmitting power allocation, and the block-length allocation among these sensor-actuator pairs. We propose an effective algorithm based on the alternating optimization technique to obtain a high-quality solution to this challenging problem. Numerical results show that the proposed algorithm achieves better performance than other benchmark schemes. Due to the space limitation, there have been some other interesting issues that are not addressed in this paper, which are discussed in the following to motivate future work.

We consider the quasi-stationary UAV scenario by only optimizing the UAV's deployment location. In some other scenarios (e.g., the IoT devices have intermittent traffics that happen at different time instants), it may be feasible to exploit the UAV's mobility over time for further enhancing the round-trip URLLC performance. In this case, how to optimize the UAV's trajectory optimization (instead of placement location only) and the wireless resource allocation to maximize the system performance is an interesting and challenging problem.

We only consider the round-trip URLLC among the sensor-actuator pairs by ignoring the computation or information pro-

▲ Figure 2. The maximum end-to-end PER versus the number of total available block-length M.
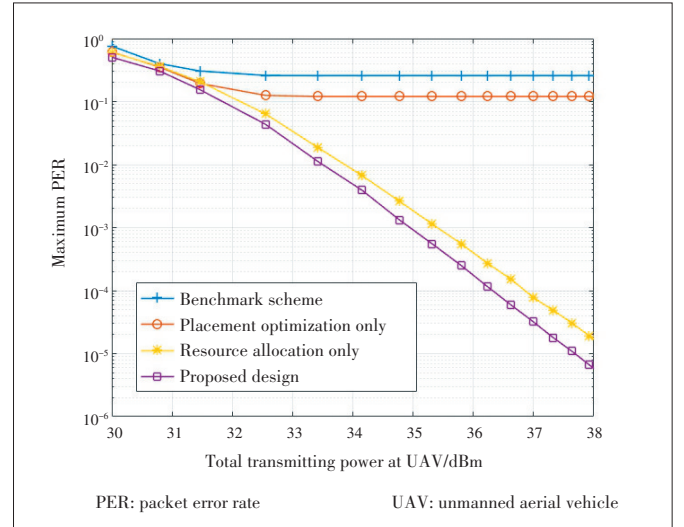
▲ Figure 3. The maximum end-to-end PER versus the UAV's maximum transmitting power P_{sum}.

cessing at the UAV. Eventually, the computation-communication tradeoff in MEC and mobile edge learning systems can also be exploited for enhancing the latency performance. How to optimize the performance of UAV-enabled MEC systems for various edge machine learning applications is an interesting direction for future investigation.

Appendix

Since $Q(x)$ is strictly decreasing and convex in x when $Q(x) < 0.5$, it suffices to show the convexity of $\varepsilon(\gamma, m)$ in γ by proving

$$f(m, \gamma) \triangleq \frac{m \ln(1 + \gamma) - N \ln 2}{\sqrt{m}\sqrt{1 - (1 + \gamma)^{-2}}}, \tag{26}$$

which is strictly concave in γ for any given m.

Let $t = 1 + \gamma > 1$, and then we have

$$\bar{f}(m,t) \triangleq f(m,\gamma) \triangleq \frac{mt\ln(t) - tN\ln2}{\sqrt{m(t^2 - 1)}}. \tag{27}$$

Thus, we have

$$\frac{\partial \bar{f}(m,t)}{\partial t} = \frac{m(t^2 - \ln t - 1) + N\ln2}{(t^2 - 1)\sqrt{m(t^2 - 1)}} =$$

$$\frac{\sqrt{m}\ (t^2 - \ln t - 1)}{(t^2 - 1)^{\frac{3}{2}}} + \frac{N\ln2}{\sqrt{m}}\frac{1}{(t^2 - 1)^{\frac{3}{2}}}. \tag{28}$$

Let $A = \sqrt{m}$, $B = \dfrac{N\ln2}{\sqrt{m}}$, we have

$$\frac{\partial^2 \bar{f}(m,t)}{\partial t^2} =$$

$$A\left(\left(2t - \frac{1}{t}\right)(t^2-1)^{-\frac{3}{2}} - 3Bt(t^2-1)^{-\frac{5}{2}} - 3t(t^2-\ln t-1)(t^2-1)^{-\frac{5}{2}}\right) \overset{\circ}{=}$$

$$\left(2t - \frac{1}{t}\right)(t^2-1) - 3t(t^2-\ln t-1) - 3t\frac{B}{A} \overset{\circ}{=} \tag{29}$$

$$\left(2 - \frac{1}{t^2}\right)(t^2+1) - 3(t^2-\ln t-1) - 3\frac{B}{A} =$$

$$-t^2 + \frac{1}{t^2} + 3\ln t - 3\frac{B}{A} < 0,$$

where $\overset{\circ}{=}$ means both sides have the same sign. Therefore, $\bar{f}(m,t)$ is concave with respect to (w.r.t.) t. Since t is the affine transformation of p, it follows that $\bar{f}(m,t)$ is also concave w.r.t. p. Due to the convexity rule of compound function[29], $\varepsilon(\gamma,m)$ is strictly convex w.r.t. p under a mild condition of $\varepsilon(\gamma,m) < 0.5$.

References

[1] MAO Y Y, YOU C S, ZHANG J, et al. A survey on mobile edge computing: the communication perspective [J]. IEEE communications surveys & tutorials, 2017, 19(4): 2322–2358. DOI:10.1109/comst.2017.2745201

[2] DING Z G, XU J, DOBRE O A, et al. Joint power and time allocation for NOMA-MEC offloading [J]. IEEE transactions on vehicular technology, 2019, 68(6): 6207–6211. DOI:10.1109/tvt.2019.2907253

[3] SUN H J, ZHOU F H, HU R Q. Joint offloading and computation energy efficiency maximization in a mobile edge computing system [J]. IEEE transactions on vehicular technology, 2019, 68(9): 3052–3056. DOI:10.1109/tvt.2019.2893094

[4] BAI T, WANG J J, REN Y, et al. Energy-efficient computation offloading for secure UAV-edge-computing systems [J]. IEEE transactions on vehicular technology, 2019, 68(6): 6074–6087. DOI:10.1109/tvt.2019.2912227

[5] WANG F, XU J, DING Z G. Multi-antenna NOMA for computation offloading in multiuser mobile edge computing systems [J]. IEEE transactions on communications, 2019, 67(3): 2450–2463. DOI:10.1109/tcomm.2018.2881725

[6] LIU J, MAO Y Y, ZHANG J, et al. Delay-optimal computation task scheduling for mobile-edge computing systems[C]//2016 IEEE International Symposium on Information Theory. Barcelona, Spain, 2016. DOI:10.1109/isit.2016.7541539

[7] WANG F, XU J, WANG X, et al. Joint offloading and computing optimization in wireless powered mobile-edge computing systems [J]. IEEE transactions on wireless communications, 2018, 17(3): 1784–1797. DOI: 10.1109/twc.2017.2785305

[8] ZHU G X, LIU D Z, DU Y Q, et al. Toward an intelligent edge: wireless communication meets machine learning [J]. IEEE communications magazine, 2020, 58(1): 19–25. DOI:10.1109/mcom.001.1900103

[9] MO X P, XU J. Energy-efficient federated edge learning with joint communication and computation design [EB/OL]. (2020–2–29)[2020–4–1]. https://arxiv.org/abs/2003.00199

[10] CUI Q M, GONG Z Z, NI W, et al. Stochastic online learning for mobile edge computing: learning from changes [J]. IEEE communications magazine, 2019, 57(3): 63–69. DOI:10.1109/mcom.2019.1800644

[11] MOTLAGH N H, BAGAA M, TALEB T. UAV-Based IoT Platform: a crowd surveillance use case [J]. IEEE Communications Magazine, 2017, 55(2): 128–134. DOI:10.1109/mcom.2017.1600587cm

[12] ZENG Y, XU J, ZHANG R. Energy minimization for wireless communication with rotary-wing UAV [J]. IEEE transactions on wireless communications, 2019, 18(4): 2329–2345. DOI:10.1109/twc.2019.2902559

[13] CAO X W, WANG F, XU J, et al. Joint computation and communication cooperation for energy-efficient mobile edge computing [J]. IEEE Internet of Things journal, 2019, 6(3): 4188–4200. DOI:10.1109/jiot.2018.2875246

[14] ZENG Y, ZHANG R, LIM T J. Wireless communications with unmanned aerial vehicles: opportunities and challenges [J]. IEEE communications magazine, 2016, 54(5): 36–42. DOI:10.1109/mcom.2016.7470933

[15] ZENG Y, ZHANG R, LIM T J. Throughput maximization for UAV-enabled mobile relaying systems [J]. IEEE transactions on communications, 2016, 64(12): 4983–4996. DOI:10.1109/tcomm.2016.2611512

[16] XU J, ZENG Y, ZHANG R. UAV-enabled wireless power transfer: trajectory design and energy optimization [J]. IEEE transactions on wireless communications, 2018, 17(8): 5092–5106. DOI:10.1109/twc.2018.2838134

[17] WU Q Q, ZENG Y, ZHANG R. Joint trajectory and communication design for multi-UAV enabled wireless networks [J]. IEEE transactions on wireless communications, 2018, 17(3): 2109–2121. DOI:10.1109/twc.2017.2789293

[18] XIE L F, XU J, ZHANG R. Throughput maximization for UAV-enabled wireless powered communication networks [J]. IEEE Internet of Things journal, 2019, 6(2): 1690–1703. DOI:10.1109/jiot.2018.2875446

[19] ZHOU F, WU Y, HU R Q, QIAN Y. Computation rate maximization in UAV-enabled wireless powered mobile-edge computing systems [J]. IEEE journal on selected areas in communications, 2018, 36(9): 1927–1941. DOI: 10.1109/JSAC.2018.2864426A

[20] GARG S, SINGH A, BATRA S, et al. UAV-empowered edge computing environment for cyber-threat detection in smart vehicles [J]. IEEE network, 2018, 32(3): 42–51. DOI:10.1109/mnet.2018.1700286

[21] PU L J, CHEN X, MAO G Q, et al. Chimera: an energy-efficient and deadline-aware hybrid edge computing framework for vehicular crowdsensing applications [J]. IEEE Internet of Things journal, 2019, 6(1): 84–99. DOI:10.1109/jiot.2018.2872436

[22] DU Y, WANG K Z, YANG K, et al. Energy-efficient resource allocation in UAV based MEC system for IoT devices [C]//2018 IEEE Global Communications Conference (GLOBECOM). Abu Dhabi, United Arab Emirates, 2018: 9–13. DOI:10.1109/glocom.2018.8647789

[23] JEONG S, SIMEONE O, KANG J. Mobile edge computing via a UAV-mounted cloudlet: optimization of bit allocation and path planning [J]. IEEE transactions on vehicular technology, 2018, 67(3): 2049–2063. DOI: 10.1109/tvt.2017.2706308

[24] ZHOU F H, WU Y P, SUN H J, et al. UAV-enabled mobile edge computing: offloading optimization and trajectory design [C]//2018 IEEE International Conference On Communications (ICC). Kansas City, USA, 2018: 20–24. DOI: 10.1109/icc.2018.8422277

[25] DURISI G, KOCH T, POPOVSKI P. Toward massive, ultrareliable, and low-latency wireless communication with short packets [J]. Proceedings of the IEEE, 2016, 104(9): 1711–1726. DOI:10.1109/jproc.2016.2537298

[26] SHEN C, CHANG T H, XU H Q, et al. Joint uplink and downlink transmission design for URLLC using finite blocklength codes [C]//2018 15th International Symposium on Wireless Communication Systems (ISWCS). Lisbon, Portugal, 2018: 28–31. DOI:10.1109/iswcs.2018.8491069